Tutkimusraportti 45

Research Report 45

A COMPUTATIONALLY EFFICIENT SHEAR DEFORMABLE BEAM ELEMENT FOR LARGE DEFORMATION MULTIBODY APPLICATIONS

Researcher, M.Sc. (Eng.) Kimmo S. Kerkkänen
Researcher, M.Sc. (Eng.) Jussi T. Sopanen
Professor, Dr. Tech. Aki M. Mikkola

ISBN 951-764-824-3 (Paperback)
ISBN 951-764-825-1 (PDF)
ISSN 1459-2932

Lappeenranta University of Technology
Department of Mechanical Engineering
Institute of Mechatronics and Virtual Engineering
P.O.Box 20
FIN-53851 Lappeenranta
Finland

Lappeenranta, October 29, 2003

Abstract

In this paper, a new two-dimensional shear deformable beam element based on the absolute nodal coordinate formulation is proposed. The nonlinear elastic forces of the beam element are obtained using a continuum mechanics approach without employing a local element coordinate system. In this study, linear polynomials are used to interpolate both the transverse and longitudinal components of the displacement. This is different from other absolute nodal-coordinate-based beam elements where cubic polynomials are used in the longitudinal direction. The accompanying defects of the phenomenon known as shear locking are avoided through the adoption of selective integration within the numerical integration method. The proposed element is verified using several numerical examples, and the results are compared to analytical solutions and the results for an existing shear deformable beam element. It is shown that by using the proposed element, accurate linear and nonlinear static deformations, as well as realistic dynamic behavior, can be achieved with a smaller computational effort than by using existing shear deformable two-dimensional beam elements.

1. Introduction

The description of nonlinear deformations is a challenging and active research topic in the area of multibody dynamics. The goal of these studies is to obtain more realistic simulation models for applications such as belts and cables. Nonlinear deformation in multibody dynamics can be treated using, for example, the absolute nodal coordinate formulation [1, 2] or the large rotation vector formulation [3]. The absolute nodal coordinate formulation has many advantages, which include the correct description of the motion of an arbitrary rigid body and a constant mass matrix. This formulation has been successfully applied to three-dimensional beams [4, 5] and shells [6]. Despite numerous investigations into the usability and accuracy of the absolute nodal coordinate formulation, there is still a need to improve its accuracy and appropriateness for computer calculation.

The objective of this investigation is to develop a new two-dimensional shear deformable beam element based on the nodal coordinate formulation where slopes and displacements are used as the nodal coordinates instead of finite or infinitesimal rotations. The proposed beam element uses a linear displacement field and a reduced amount of slope coordinates in comparison to the previously introduced absolute nodal coordinate finite elements. The smaller number of nodal coordinates leads to a reduced degree of freedom in the finite element, which leads to computational advantages in structural analysis.

Using the absolute nodal coordinate formulation, the global position vector, $\mathbf{r}$, of an arbitrary point in a planar case can be written as

$$\mathbf{r} = \mathbf{S}(x, y)\mathbf{e}, \tag{1}$$

where $\mathbf{S}$ is the element shape function matrix, x and y are the local coordinates of the element and $\mathbf{e}$ is the vector of the nodal coordinates. The assumed displacement field of the two-dimensional shear deformable element can be defined in a global coordinate system by using the following polynomial expression [7, 8]:

$$\mathbf{r} = \begin{bmatrix} r_1 \\ r_2 \end{bmatrix} = \begin{bmatrix} a_0 + a_1x + a_2y + a_3xy + a_4x^2 + a_5x^3 \\ b_0 + b_1x + b_2y + b_3xy + b_4x^2 + b_5x^3 \end{bmatrix} \tag{2}$$

The assumed displacement field in Eq. (2) includes 12 unknown polynomial coefficients. For this reason, six nodal coordinates are needed for each node for a two-noded (*I, J*) beam element. In this case, the nodal coordinates, $\mathbf{e}_I$, can be written as

$$\mathbf{e}_I = \begin{bmatrix} \mathbf{r}_I^T & \dfrac{\partial \mathbf{r}_I^T}{\partial x} & \dfrac{\partial \mathbf{r}_I^T}{\partial y} \end{bmatrix}^T, \tag{3}$$

where $\mathbf{r}_I$ is the global position vector of node *I* and vectors $\partial \mathbf{r}_I^T / \partial x$ and $\partial \mathbf{r}_I^T / \partial y$ are the slopes of node *I*. Vector $\partial \mathbf{r}_I^T / \partial x$ defines the global orientation of the centerline of the beam and vector $\partial \mathbf{r}_I^T / \partial y$ defines the orientation of the height coordinates of the cross-section of the beam [9].

2. Kinematics of the Proposed Element

In this chapter, the kinematics of the proposed beam element is introduced. The proposed beam element uses linear polynomials to interpolate both the transverse and longitudinal components of displacement, and the slope coordinates, $\partial \mathbf{r}^T / \partial x$, are neglected. The reduced amount of nodal coordinates produces a smaller degree of freedom in each node of the finite element.

The assumed displacement field of the two-dimensional shear deformable element can be defined in a global coordinate system using the following linear polynomial expression:

$$\mathbf{r} = \begin{bmatrix} r_1 \\ r_2 \end{bmatrix} = \begin{bmatrix} a_0 + a_1x + a_2y + a_3xy \\ b_0 + b_1x + b_2y + b_3xy \end{bmatrix} \tag{4}$$

Eq. (4) includes eight unknown polynomial coefficients. Four nodal coordinates can be chosen for each node of a two-noded beam element as follows:

$$\mathbf{e}_I = \begin{bmatrix} \mathbf{r}_I^T & \dfrac{\partial \mathbf{r}_I^T}{\partial y} \end{bmatrix}^T . \tag{5}$$

The element shape function matrix, **S**, can be expressed by using the nodal coordinates and the interpolating polynomial of Eq. (4) as follows:

$$\mathbf{S} = \begin{bmatrix} S_1\mathbf{I} & S_2\mathbf{I} & S_3\mathbf{I} & S_4\mathbf{I} \end{bmatrix} \tag{6}$$

In Eq. (6), **I** is a 2 × 2 identity matrix and the element shape functions, $S_1 \ldots S_4$, are

$$S_1 = 1 - \xi, \qquad S_2 = l(\eta - \xi\eta), \qquad S_3 = \xi, \qquad S_4 = l\xi\eta,$$

where l is the length of the element in the initial configuration and the non-dimensional quantities, ξ and η, are defined as

$$\xi = \frac{x}{l}, \qquad \eta = \frac{y}{l}$$

The shape functions contain only one quadratic term, xy, while the remaining shape functions are products of one-dimensional linear polynomials.

3. The elastic Forces of the Beam Element

The definition of the elastic forces for the absolute nodal coordinate beam element can be obtained by using a continuum mechanics approach [7, 10]. In this investigation, a nonlinear expression is employed for the elastic forces. The gradient of the displacement vector can be defined as

$$\mathbf{D} = \frac{\partial \mathbf{r}}{\partial \mathbf{x}} \left(\frac{\partial \mathbf{X}}{\partial \mathbf{x}} \right)^{-1} = \frac{\partial (\mathbf{S}\mathbf{e})}{\partial \mathbf{x}} \left[\frac{\partial (\mathbf{S}\mathbf{e}_0)}{\partial \mathbf{x}} \right]^{-1} = \mathbf{J}\mathbf{J}_0^{-1}. \tag{7}$$

In Eq. (7), **X** and **x** are the vectors of the global and local element coordinates, respectively. The vectors of the nodal coordinates in the deformed and initial configuration are presented by $\mathbf{e}$ and $\mathbf{e}_0$. Matrix $\mathbf{J}$ is the deformation gradient and matrix $\mathbf{J}_0$ a constant transformation matrix. If the element has an arbitrary initial configuration, matrix $\mathbf{J}_0$ must be taken into account in the formulation of the elastic forces. Matrix $\mathbf{J}_0$ is the identity matrix in the case of a straight element.

The Green Lagrange strain tensor, $\boldsymbol{\varepsilon}_m$, can be written using the right Cauchy-Green deformation tensor as follows:

$$\boldsymbol{\varepsilon}_m = \frac{1}{2}\left(\mathbf{D}^T\mathbf{D} - \mathbf{I}\right) \tag{8}$$

The strain tensor of $\boldsymbol{\varepsilon}_m$ is symmetric, and therefore, only three strain components are needed to identify it and these components can be written in vector form as

$$\boldsymbol{\varepsilon} = \begin{bmatrix} \varepsilon_{m_{11}} & \varepsilon_{m_{22}} & 2\varepsilon_{m_{12}} \end{bmatrix}^T . \tag{9}$$

Using matrix $\mathbf{E}$, which contains the elastic coefficients of the material, the expression of the strain energy can be written as follows:

$$U = \frac{1}{2}\int_V \boldsymbol{\varepsilon}^T \mathbf{E} \boldsymbol{\varepsilon} \, dV \tag{10}$$

Matrix $\mathbf{E}$ can be expressed for an isotropic homogenous material in terms of Lame's constants, λ and μ, as follows:

$$\mathbf{E} = \begin{bmatrix} \lambda + 2\mu & \lambda & 0 \\ \lambda & \lambda + 2\mu & 0 \\ 0 & 0 & \mu \end{bmatrix} \tag{11}$$

In Eq. (11), $\lambda = E\nu/[(1+\nu)(1-2\nu)]$ and $\mu = E/[2(1+\nu)]$, where E is Young's modulus of elasticity and ν the Poisson's ratio of the material.

By neglecting the Poisson's effect, the strain energy, U, can be written using Young's modulus of elasticity, E, and shear modulus, G, as follows [11]:

$$U = \frac{1}{2}\int_V \left(E\varepsilon_{m_{11}}^2 + E\varepsilon_{m_{22}}^2 + 4k_s G\varepsilon_{m_{12}}^2 \right) dV \tag{12}$$

In order to obtain the correct shear strain energy, the shear correction factor, k_s, is needed to minimize the error between the constant and the known true parabolic shear strain contributions.

The vector of the elastic forces, $\mathbf{Q}_e$, can be defined as the derivative of the strain energy expression with respect to the element nodal coordinate vector as follows:

$$\mathbf{Q}_e = \left(\frac{\partial U}{\partial \mathbf{e}} \right)^T \tag{13}$$

The mass matrix given by the absolute nodal coordinate formulation is constant and symmetric. Using the element shape function given by Eq. (6), the mass matrix, $\mathbf{M}$, can be written as

$$\mathbf{M} = \int_V \rho \mathbf{S}^T \mathbf{S} \, dV \,, \tag{14}$$

where ρ and V are the mass, density and volume of the finite element, respectively.

4. Generalization to a Three-Dimensional Shear Deformable Beam Element

The generalization of the proposed two-dimensional shear deformable beam element for three-dimensional problems is straightforward. Using the absolute nodal coordinate formulation, the global position vector, **r**, of an arbitrary point in a spatial case can be written as

$$\mathbf{r} = \mathbf{S}(x, y, z)\mathbf{e}\,, \tag{15}$$

where **S** is the element shape function matrix, x, y and z are the local coordinates of the element and **e** is the vector of the nodal coordinates. By neglecting the higher-order terms from the assumed displacement field, the assumed displacement field of the three-dimensional shear deformable element can be defined in a global coordinate system using the following polynomial expression:

$$\mathbf{r} = \begin{bmatrix} r_1 \\ r_2 \\ r_3 \end{bmatrix} = \begin{bmatrix} a_0 + a_1x + a_2y + a_3z + a_4xy + a_5xz \\ b_0 + b_1x + b_2y + b_3xy + b_4xy + b_5xz \\ c_0 + c_1x + c_2y + c_3xy + c_4xy + c_5xz \end{bmatrix} \tag{16}$$

Eq. (16) includes 18 unknown polynomial coefficients. Nine nodal coordinates can be chosen for each node of a two-node beam element as follows:

$$\mathbf{e}_I = \begin{bmatrix} \mathbf{r}_I^T & \dfrac{\partial \mathbf{r}_I^T}{\partial y} & \dfrac{\partial \mathbf{r}_I^T}{\partial z} \end{bmatrix}, \tag{17}$$

where vector $\partial \mathbf{r}_I^T / \partial z$ defines the orientation of the width coordinates of the cross-section of the beam [9].

The element shape function matrix, **S**, can be expressed by using the nodal coordinates and the interpolating polynomial of Eq. (16) as follows:

$$\mathbf{S} = \begin{bmatrix} S_1\mathbf{I} & S_2\mathbf{I} & S_3\mathbf{I} & S_4\mathbf{I} & S_5\mathbf{I} & S_6\mathbf{I} \end{bmatrix} \tag{18}$$

In Eq. (18), **I** is a 3 × 3 identity matrix and the element shape functions $S_1 \ldots S_6$ are

$$S_1 = 1 - \xi, \qquad S_2 = l(\eta - \xi\eta), \qquad S_3 = l\zeta(1-\xi),$$

$$S_4 = \xi, \qquad S_5 = l\xi\eta, \qquad S_6 = l\xi\zeta,$$

where l is the length of the element in the initial configuration and the non-dimensional quantities ξ, η and ζ are defined as follows:

$$\xi = \frac{x}{l}, \qquad \eta = \frac{y}{l}, \qquad \zeta = \frac{z}{l}$$

The shape functions contain both quadratic terms and terms that are products of one-dimensional linear polynomials.

5. Selective Integration of the Strain Energy

The shape functions of the proposed two-dimensional shear deformable beam element include only one non-linear term, xy. Therefore, the element is able to exhibit only a rectangular deformation shape. This characteristic results in parasitic shear strain under pure bending. As a result, the element stores excess shear strain energy that leads to a phenomenon called shear locking, as shown in Fig. 1 [12]. This phenomenon is encountered when using the exact integration of all the integrals of the strain energy. In this case, the model is not able to receive analytical values of displacement, even if hundreds elements are used. Especially in cases of thin beam structures, element shear locking results in overly small displacement in comparison to the exact values.

To avoid the accompanying defects of spurious shear strain, selective integration is adopted within the numerical integration method. In this case, one Gauss point is used to evaluate the contribution of shear strain in the equation of strain energy, while two Gauss points are used to evaluate the contribution of normal strains.

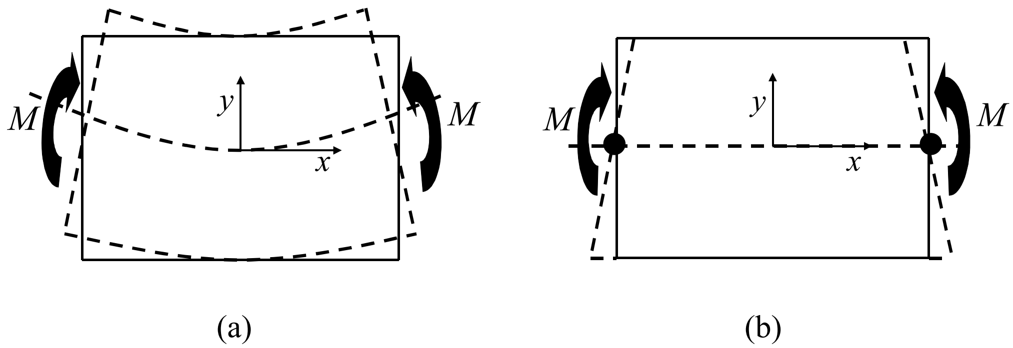

Figure 1. **(a) The correct deformation mode of a rectangular block in pure bending.**
(b) The shear locking of the element results in the incorrect deformation mode of a rectangular block in pure bending.

6. Equations of Motion

Using the constant mass matrix and the elastic force vector, which is a nonlinear function when the absolute nodal coordinates are used, the equations of motion of the deformable finite element can be written as [1]

$$\mathbf{M}\ddot{\mathbf{e}} = \mathbf{Q}_e - \mathbf{Q}_k \ , \tag{19}$$

where $\mathbf{Q}_k$ is the vector of the generalized external nodal forces including gravity forces. Using force vector $\mathbf{Q} = \mathbf{Q}_e - \mathbf{Q}_k$, the preceding equation takes the following form:

$$\mathbf{M}\ddot{\mathbf{e}} = \mathbf{Q} \tag{20}$$

Since the mass matrix is a constant matrix, the vector of the accelerations $\ddot{\mathbf{e}}$ of Eq. (20) can be efficiently solved using numerical procedures on the following equation:

$$\ddot{\mathbf{e}} = \mathbf{M}^{-1}\mathbf{Q} \tag{21}$$

The kinematic constraints that depend on the nodal coordinates and possibly on time in the multibody system can be written in vector form as [13]

$$\mathbf{C}(\mathbf{e},t)=\mathbf{0}, \tag{22}$$

where $\mathbf{C}$ is the vector of linearly independent constraint equations, $\mathbf{e}$ the nodal coordinate vector and t time.

The equation of motion that takes into account the effect of the constraints can be defined using Lagrange's equation in matrix form as follows:

$$\mathbf{M}\ddot{\mathbf{e}}+\mathbf{C}_{\mathbf{e}}^{T}\boldsymbol{\lambda}=\mathbf{Q}_{e}-\mathbf{Q}_{k}+\mathbf{Q}_{v} \tag{23}$$

In Eq. (23), $\mathbf{C}_{\mathbf{e}}^{T}$ is the Jacobian matrix that is the partial derivative of the constraint vector with respect to nodal coordinate vector, $\boldsymbol{\lambda}$ is the vector of Lagrange multipliers and $\mathbf{Q}_{v}$ is a quadratic velocity vector. The unknowns $\boldsymbol{\lambda}$ and $\ddot{\mathbf{e}}$ of Eq. (23) can be determined by differentiating the constraints of Eq. (22) twice with respect to time:

$$\mathbf{C}_{\mathbf{e}}\ddot{\mathbf{e}}\;=-\mathbf{C}_{tt}-(\mathbf{C}_{\mathbf{e}}\dot{\mathbf{e}})_{\mathbf{e}}\dot{\mathbf{e}}-2\mathbf{C}_{\mathbf{e}t}\dot{\mathbf{e}}\;=\mathbf{Q}_{c} \tag{24}$$

and writing a system of differential and algebraic equations in matrix form as follows:

$$\begin{bmatrix}\mathbf{M} & \mathbf{C}_{\mathbf{e}}^{T}\\ \mathbf{C}_{\mathbf{e}} & \mathbf{0}\end{bmatrix}\begin{bmatrix}\ddot{\mathbf{e}}\\ \boldsymbol{\lambda}\end{bmatrix}=\begin{bmatrix}\mathbf{Q}_{e}-\mathbf{Q}_{k}+\mathbf{Q}_{v}\\ \mathbf{Q}_{c}\end{bmatrix} \tag{25}$$

7. Numerical Results

In this section, the performance of the proposed shear deformable beam element is investigated in static and dynamic problems. In the static problems, the simple beam structures of Figs. 2…4 are investigated. The cross-section of the beam is rectangular and the length of the beam 2.0 m. The material of the structure is assumed to be isotropic, the Young's modulus of the material is $2.07\cdot10^{11}$ N/m^2 and mass density 7850 kg/m^3. The results of the examples for the proposed beam element are compared to those of the analytical solutions and/or to the solution from a commercial finite element code ANSYS and a two-dimensional shear deformable beam element proposed by Omar and Shabana [7]. The strain energy of the proposed beam element is calculated using Eq. (12) with a shear correction factor $k_s = 5/6$. Eq. (10) is used to determine the strain energy in the case of the element proposed by Omar and Shabana.

In the first example, the linear deformations are considered using the simply supported beam structure of Fig. 2. The boundary conditions are given to eliminate the x and y displacements of the first node and the y displacement of the last node. The cross-section of the beam is a 0.1-m-sided square and a vertical load, $F = 1000$ N, is applied to the mid-point of the beam. The vertical displacements of the midpoint are investigated using different numbers of elements for two values of the Poisson's ratio, 0.0 and 0.3. In the analytical solution and in the BEAM3 model in ANSYS [14], the effect of the shear force is considered. The results of the first example are shown in Tables 1 and 2.

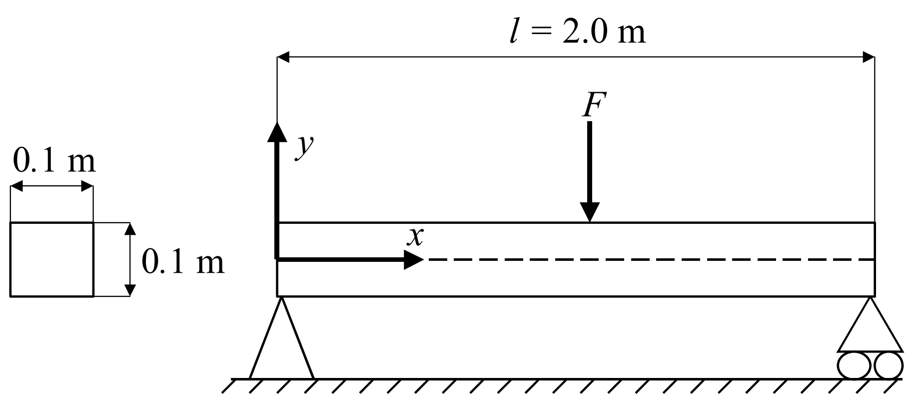

Figure 2. A simply supported beam for linear deformations.

Table 1. The vertical positions of the mid-point of the beam for a Poisson's ratio of 0.0

Number of elements	Mid-point vertical position [mm]		
	The ANCF 2D beam element of Omar and Shabana	**Proposed ANCF 2D beam element**	**ANSYS: BEAM3**
2	-0.07289318	-0.07304348	-0.097021
4	-0.09103438	-0.09115942	-0.097021
8	-0.09557755	-0.09568840	-0.097021
16	-0.09671692	-0.09682065	-0.097021
32	-0.09700354	-0.09710371	-0.097021
64	-0.09707761	-0.09717448	-0.097021
The analytical result: -0.09719807			

Table 2. The vertical positions of the mid-point of the beam for a Poisson's ratio of 0.3

Number of elements	Mid-point vertical position [mm]		
	The ANCF 2D beam element of Omar and Shabana	**Proposed ANCF 2D beam element**	**ANSYS: BEAM3**
2	-0.05438847	-0.07321739	-0.097142
4	-0.06787886	-0.09133333	-0.097142
8	-0.07126169	-0.09586232	-0.097142
16	-0.07211204	-0.09699456	-0.097142
32	-0.07232694	-0.09727763	-0.097142
64	-0.07238182	-0.09734839	-0.097142
The analytical result: -0.0972850			

It can be seen in Table 1 that in the case of a Poisson's ratio of zero, all the models agree well with each other. The proposed beam element predicts the most accurate results in comparison to the analytical result, while the BEAM3 model predicts the most underestimated displacement. In the proposed element, the bending moment is constant as is also the case of the beam element of Omar and Shabana. For this reason, these elements give more accurate results when the number of elements is increased. Table 2 shows that when the Poisson's ratio of the material is non-zero, the model by Omar and Shabana suffers from residual transverse normal stresses [9], which leads to notably smaller deformations in comparison to the results of the other models. The proposed beam element converges to slightly larger deformations than the analytical solution, which demonstrates slightly excessive flexible behavior.

In the second example, large nonlinear deformations of the simple cantilever structure of Fig. 3 are considered and compared to the nonlinear solution of the BEAM188 model in ANSYS [9, 14]. The other end of the beam is clamped by boundary conditions that eliminate the x and y displacement and slopes $\partial \mathbf{r}_1 / \partial y$ and $\partial \mathbf{r}_2 / \partial y$ of the first node. The vertical displacements of the endpoint are investigated using different numbers of elements for the two different cantilever models: In the first model (Model 1), the beam has a 0.1-m-sided square cross-section and value of the Poisson's ratio is 0.3, while in the second model (Model 2), the height h of the beam is increased from 0.1 m to 0.5 m while the Poisson's ratio is 0.0. A vertical force, $F = -5.0 \cdot 10^8 \cdot h^3$ N, is applied to the free end of the cantilever. The results of the second problem are shown in Tables 3 and 4.

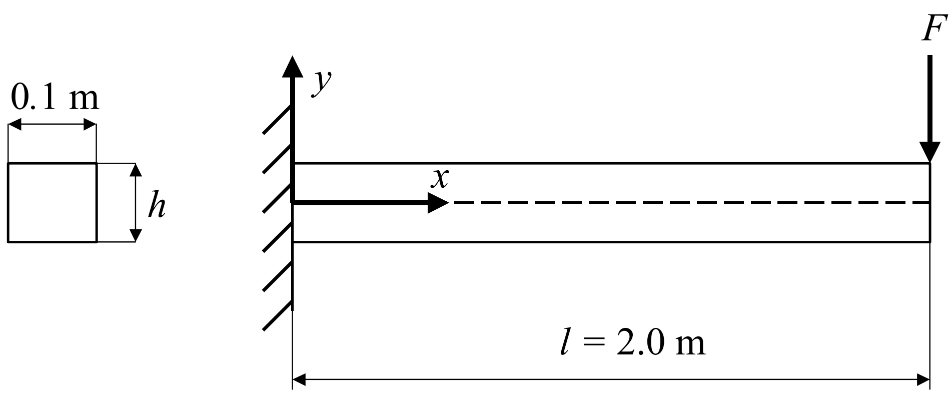

Figure 3. The cantilever beam model for nonlinear deformations.

Table 3. The beam endpoint positions in Model 1.

Number of elements	Tip Position (x, y), [m]		
	The ANCF 2D beam element of Omar and Shabana	**Proposed ANCF 2D beam element**	**ANSYS: BEAM188**
2	1.95536, -0.37731	1.93097 -0.47477	1.87080, -0.65671
4	1.91696, -0.50935	1.86837 -0.64974	1.85918, -0.67485
8	1.91342, -0.53039	1.85667 -0.67758	1.85618, -0.67947
16	1.91274, -0.53271	1.85526 -0.68046	1.85540, -0.68069
32	1.91262, -0.53313	1.85497 -0.68100	1.85520, -0.68100
64	1.91259, -0.53323	1.85489 -0.68114	1.85515, -0.68108

As can be seen in Table 3, in the case of Model 1 the beam element of Omar and Shabana suffers from residual transverse normal stresses. The predicted displacements of the proposed model and the BEAM188 model are very similar with the exception of the case of two elements.

Table 4. The beam endpoint positions in Model 2.

Number of elements	Tip Position (*x*, *y*), [m]		
	The ANCF 2D beam element of Omar and Shabana	**Proposed ANCF 2D beam element**	**ANSYS: BEAM188**
2	1.86888, -0.64147	1.87049 -0.65646	1.86749, -0.67783
4	1.84807, -0.69512	1.84801 -0.70045	1.85551, -0.69700
8	1.84462, -0.70421	1.84334 -0.70883	1.85246, -0.70179
16	1.84371, -0.70654	1.84204 -0.71123	1.85169, -0.70299
32	1.84341, -0.70725	No convergence	1.85150, -0.70329
64	1.84330, -0.70750	No convergence	1.85145, -0.70337

Table 4 shows that in the case of Model 2, the beam element of Omar and Shabana and the BEAM188 model are in good agreement but the proposed beam element fails in convergence when 32 or more elements are used. It was also noticed that if the Poisson's ratio was changed to 0.3 or the height of the beam decreased, for example, to 0.4 m, the convergence of the beam element improved. When a small number of proposed elements is used, the model converges to larger deformations than do the other models. These results can be explained as a consequence of using reduced integration in the selective integration of the strain components of the element. Reduced integration has a softening effect and may also introduce some spurious modes, such as zero-energy deformation modes or hourglass modes. The spurious modes incorporated by the stiffness matrix of the element can deactivate the resistance to nodal loads. As a result, spurious zero energy modes are activated in the element [12]. The convergence problem is solved by increasing the number of Gauss points from one to two when evaluating the contribution of the *y*-component of the shear strain in the strain energy equation. The results achieved by this modification are shown in Table 5. The softening effect of the reduced integration can still be observed in the proposed element.

Table 5. The positions of the beam endpoint in Model 2.

Number of elements	Tip Position (X, Y), [m]		
	The ANCF 2D beam element of Omar and Shabana	**Proposed ANCF 2D beam element**	**ANSYS: BEAM188**
2	1.86888, -0.64147	1.87066 -0.65601	1.86749, -0.67783
4	1.84807, -0.69512	1.84801 -0.70045	1.85551, -0.69700
8	1.84462, -0.70421	1.84343 -0.70861	1.85246, -0.70179
16	1.84371, -0.70654	1.84228 -0.71066	1.85169, -0.70299
32	1.84341, -0.70725	1.84198 -0.71119	1.85150, -0.70329
64	1.84330, -0.70750	1.84191 -0.71133	1.85145, -0.70337

In the third example, the linear axial deformations of the simple cantilever structure of Fig. 4 are considered and compared to the ANSYS BEAM3 model and analytical results. The other end of the beam is pinned by eliminating the x and y displacement of the first node. The beam has a 0.1-m-sided square cross-section. A horizontal force, F = 50 000 N, is applied to the free end of the cantilever. The elongation of the cantilever is investigated for two values of the Poisson's ratio, 0.0 and 0.3. The results are independent of the numbers of elements and are shown in Table 6. The results are almost identical with the exception of the case of the beam element by Omar and Shabana with a Poisson's ratio of 0.3.

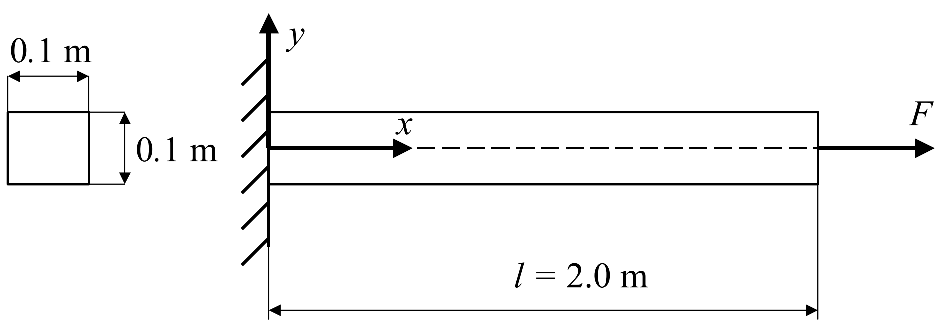

Figure 4. The cantilever beam model for linear axial deformations.

Table 6. The elongation of the beam in the *x*-direction.

Model	The elongation of the beam [mm]
Analytical (Poisson's ratio 0.0 and 0.3)	0.048309
ANSYS BEAM3 (Poisson's ratio 0.0 and 0.3)	0.048309
The ANCF 2D beam element of Omar and Shabana (Poisson's ratio 0.3)	0.043960
The ANCF 2D beam element of Omar and Shabana (Poisson's ratio 0.0)	0.048307
Proposed ANCF 2D beam element (Poisson's ratio 0.3 and 0.0)	0.048307

In the dynamic problem, the dynamic behavior of a simple planar pendulum, which consists of one beam, shown in Fig. 5, is investigated using different numbers of proposed two-node two-dimensional shear deformable beam elements. The pendulum is connected to the ground by a revolute joint, and the only force acting on the system is gravity, which is equal to 9.81 m/s^2. The cross-section of the beam is a 0.1-m-sided square, while the length of the beam is 2.0 m. The material of the structure is assumed to be isotropic and the Young's modulus of the material is $2.07 \cdot 10^7$ N/m^2, the Poisson's ratio 0.3 and mass density 7850 kg/m^3.

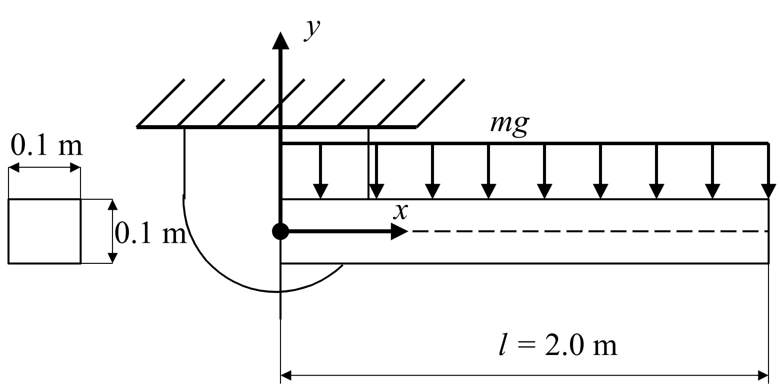

Figure 5. A free falling flexible pendulum for dynamic verification in the initial position.

The initial position of the beam is horizontal with an initial velocity of zero. The vertical displacement of the beam endpoint for different numbers of elements is shown in Fig. 6.

As can be seen, the solutions for 8 and 16 elements are almost identical and the solution for 4 elements is in good agreement with them.

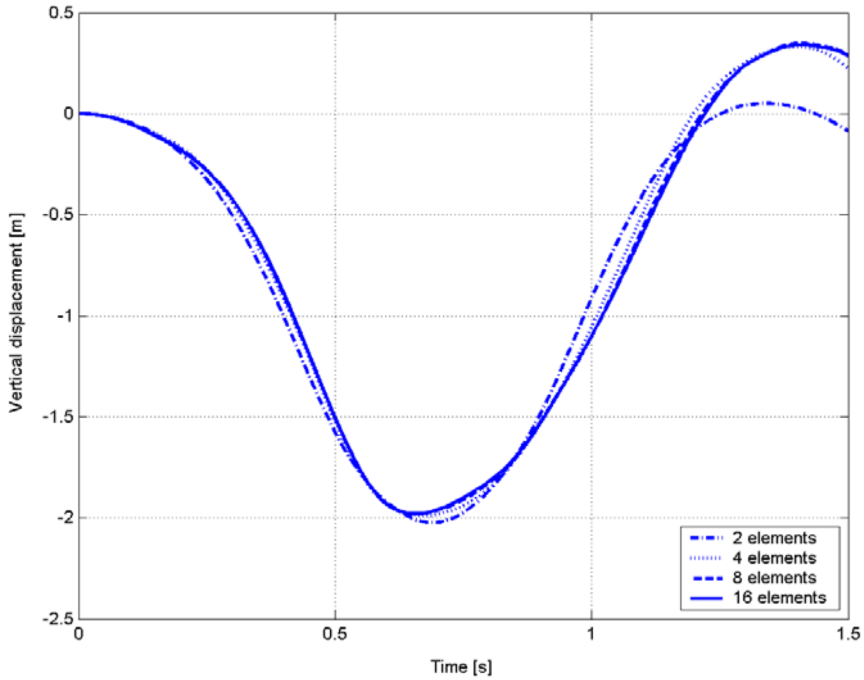

Figure 6. Vertical displacement of the falling flexible beam tip point using 2, 4, 8 and 16 elements.

The energy balance of the beam should remain constant due to the fact that the free-falling pendulum is a conservative system. This can be written as

$$\sum_{i}^{n}\left(T^{i}+V^{i}+U^{i}\right)=\text{constant}\,, \tag{26}$$

where n is the number of elements of the system, T^i the kinetic energy, V^i the potential energy and U^i the strain energy of the element [10]. The energy components of the beam made up of 4 elements are shown in Fig. 7. It can be seen that the energy balance remains constant with excellent accuracy. Fig. 8 shows the linear behavior of the proposed beam element in the case of large deformations of the falling beam made up of 6 elements. The proposed elements remain straight due to the use of linear polynomials to interpolate the displacement components.

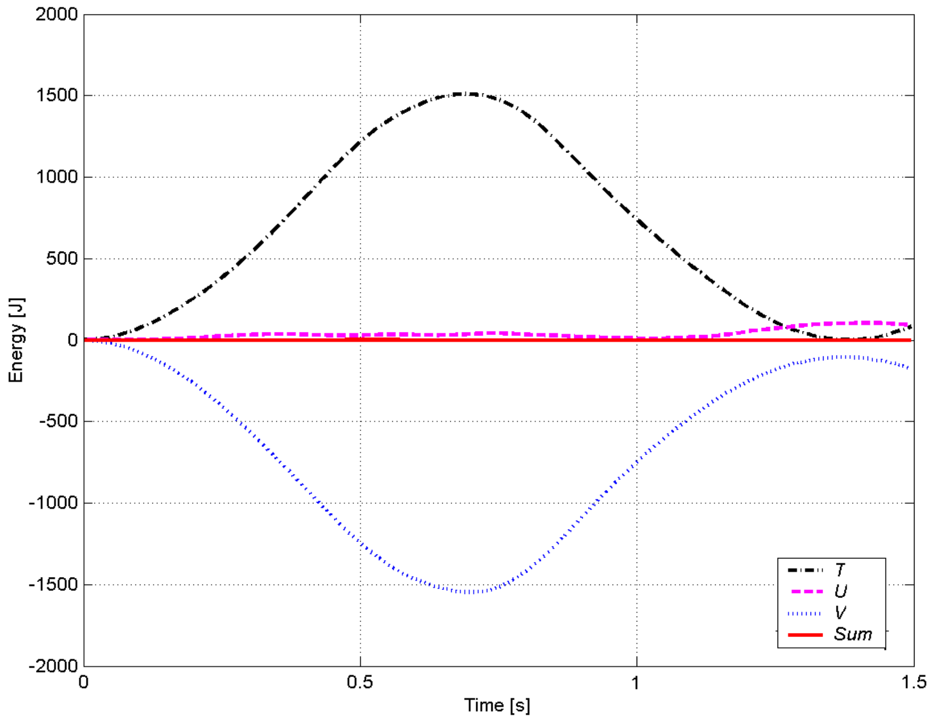

Figure 7. The energy components and energy balance of the falling flexible beam made up of 4 elements.

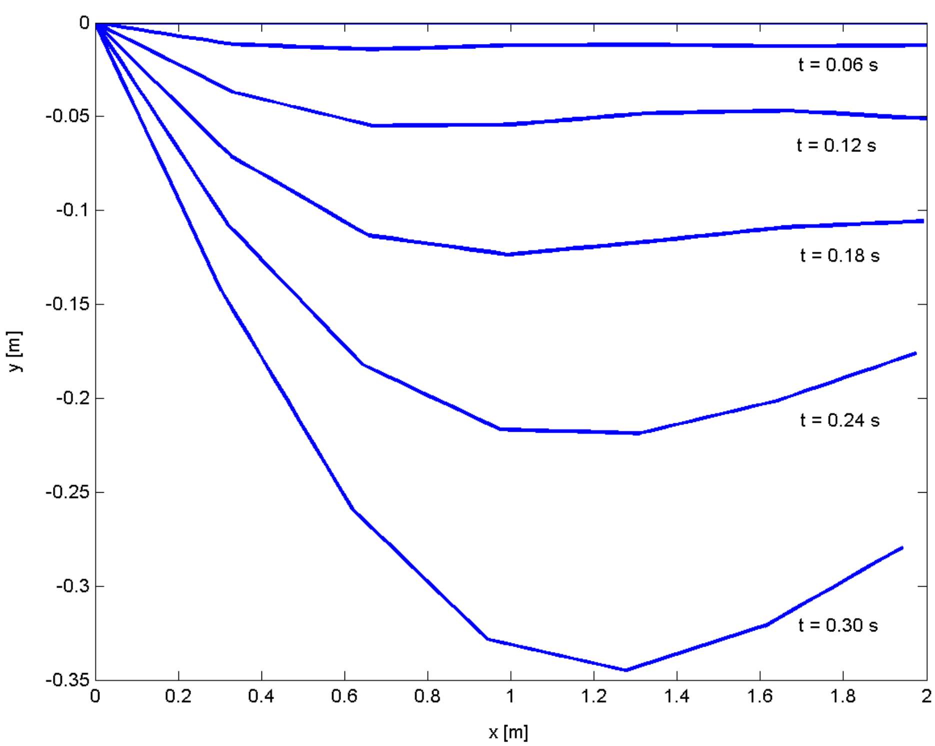

Figure 8. The falling flexible pendulum at different time steps under the effect of gravity using 6 elements.

A comparison of the vertical displacement between the proposed element and that presented by Omar and Shabana is shown in Fig. 9. The results are obtained using 4 elements and moderate agreement can be observed between the models. The differences between the results are reduced if the number of elements in the models is increased as shown in Fig. 10. Using the proposed beam element, a significant saving in computation time can be achieved in comparison to using the beam element presented by Omar and Shabana. This is due to the fact that less nodal coordinates and simpler polynomials are needed to identify the element, and the dimensions of the vectors and matrices in the calculation are smaller.

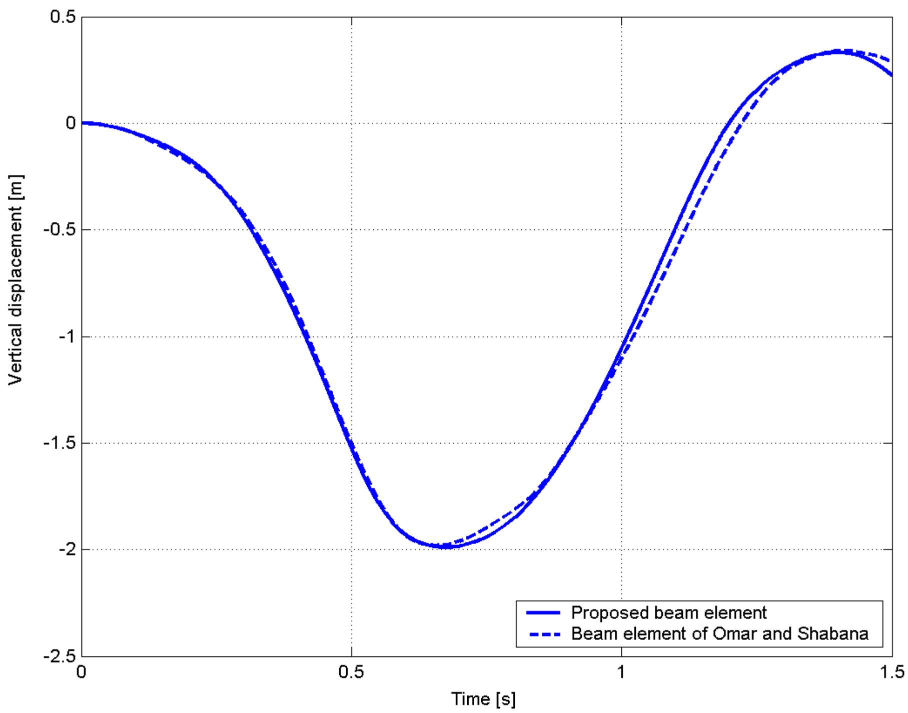

Figure 9. A comparison of the vertical displacement between the proposed element and that presented by Omar and Shabana using 4 elements.

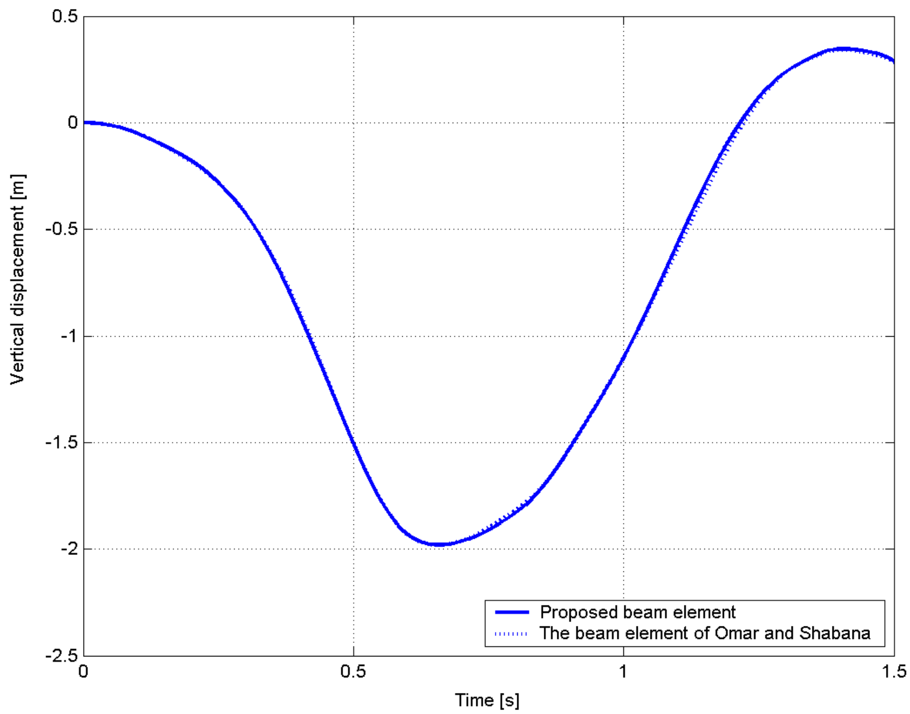

Figure 10. A comparison of the vertical displacement between the proposed element and that presented by Omar and Shabana using 8 elements.

8. Conclusions

It has been perceived that although the displacement field of the element includes a cubic interpolation polynomial in the axial direction of the displacement, the element exhibits linear bending behavior when a continuum mechanics approach is used. For this reason, the advantage of the third-order polynomial expansion is debatable.

The objective of this investigation was to develop a computationally efficient two-dimensional shear deformable beam element based on the absolute nodal coordinate formulation. The beam element uses a linear displacement field neglecting higher-order terms and a reduced number of nodal coordinates, which leads to fewer degrees of freedom in a finite element. The expression of the elastic forces is nonlinear. The accompanying defects of the phenomenon known as shear locking are avoided through the adoption of selective integration within the numerical integration method.

Several numerical examples, including both static and dynamic tests, were used to demonstrate the functionality and usability of the proposed beam model. The results were compared to the results of a commercial finite element code ANSYS, the results of the previously published beam element model by Omar and Shabana and analytical results. Generally the results, in the cases of linear and non-linear deformations, are in good agreement. For non-linear deformations, the discrepancies between the different models increased when the height of the beam was increased, which increased the significance of the role of shear strain.

It was perceived that the proposed beam element experiences problems in convergence when the number of elements is increased for the non-linear deformation test excluding the case of a relatively thin beam. It is shown in this investigation that the convergence problem can be solved by increasing the number of Gauss points from one to two when evaluating the contribution of the y-component of shear strain. In the case of a simple pendulum, the results of the proposed beam element demonstrate good functionality. The energy balance of the dynamic model remains exactly constant, and the results are in good agreement with the beam model of Omar and Shabana with less computational effort.

References

[1] Shabana, A. A., 1998, *Dynamics of Multibody Systems,* John Wiley & Sons, New York.

[2] Shabana, A. A., 1998, "Computer Implementation of the Absolute Nodal Coordinate Formulation for Flexible Multibody Dynamics", *Nonlinear Dynamics*, **16**, pp. 293-306.

[3] Cardona, A., and Geradin, M., 1988, "A Beam Finite Element Non-Linear Theory with Finite Rotations", *International Journal for Numerical Methods in Engineering,* **26**, pp. 2403-2438.

[4] Shabana, A. A., and Yakoub, R. Y., 2001, "Three Dimensional Absolute Nodal Coordinate Formulation for Beam Elements: Theory", *ASME Journal of Mechanical Design*, **123**, pp. 606-613.

[5] Yakoub, R. Y., and Shabana, A. A., 2001, "Three Dimensional Absolute Nodal Coordinate Formulation for Beam Elements: Implementation and application", *ASME Journal of Mechanical Design*, **123**, pp. 614-621.

[6] Mikkola, A. M., and Shabana, A. A, 2003, " A Non-Incremental Finite Element Procedure for the Analysis of Large Deformation of Plates and Shells in Mechanical System Applications", *Multibody System Dynamics*, **9**, pp. 283-309.

[7] Omar, M. A., and Shabana, A. A., 2001, "A Two-Dimensional Shear Deformation Beam for Large Rotation and Deformation", *Journal of Sound and Vibration*, **243**(3), pp. 565-576.

[8] Escalona, J. L., Hussien H. A., and Shabana A. A., 1998, "Application of the Absolute Nodal Coordinate Formulation to Multibody System Dynamics", *Journal of Sound and Vibration*, **214**(5), pp. 833-851.

[9] Sopanen, J. T., and Mikkola, A. M., 2003, "Studies on the stiffness properties of the absolute nodal coordinate formulation for three-dimensional beams", *in Proceedings of ASME 2003 Design Engineering Conferences and Information in Engineering Conference,* DETC2003/VIB-48325.

[10] Berzeri, M., and Shabana, A. A., 2000 "Development of Simple Models for The Elastic Forces of The Absolute Nodal Coordinate Formulation", *Journal of Sound and Vibration*, **235**(4), pp. 539-565.

[11] Sharf, I., 1999, "Nonlinear Strain Measures, Shape Functions and Beam Elements for Dynamics of Flexible Beams", *Multibody System Dynamics*, **3**, pp. 189-205.

[12] Cook, R. D., 1981, *Concepts and applications of finite element analysis*, Wiley, New York.

[13] Shabana, A. A., 1994, *Computational dynamics*, Wiley, New York.

[14] ANSYS User's Manual, 2001, Theory, Twelfth Edition, SAS IP, Inc. ©.